Look-up Table-Based Simulation of Scintillation Detectors in Computed Tomography

Michael Balda, Stefan Wirth, Daniel Niederlöhner, Björn Heismann and Joachim Hornegger

***Abstract*—The design of a CT detector requires a precise detector model, since building prototypes for many different proposed detector geometries is too costly. We introduce a look-up table-based simulation of scintillation detectors on X-ray photon level. It uses energy-resolved sinograms of incoming X-ray intensities as input data and generates photon counts for each channel and reading. The effects of X-ray- and optical cross-talk, temporal cross-talk between readings, Poisson noise and electronics effects are covered. The photon interaction data as well as optical cross-talk distribution are provided in the form of detector specific look-up tables. Unlike standard Monte-Carlo simulations of X-ray interaction processes, our approach is capable of simulating whole sinograms in a reasonable amount of time and still offers a very high precision of the detector model. This way the influence of detector effects can be investigated in the reconstructed image data. The simulation is verified against data measured with a CT scanner and data from a fully single photon-based Monte-Carlo simulation in terms of image modulation transfer function (MTF) and detector noise power spectrum (NPS).**

I. Introduction

Scintillation detectors are the current state of the art technology for CT systems. CT detectors are constantly improved in terms of resolution, coverage and signal quality to provide better images and a broader range of applicability. The development of a new detector requires precise evaluation of proposed designs, so that properties like pixel- and septa-size can be adjusted. As building detector prototypes is very expensive, the evaluation of many parameters relies on simulations. For this purpose, an efficient and precise detector simulation is needed.

Figure 1 shows a basic layout of the detector. In the scintillator material incoming X-ray photons are converted to optical photons. The optical photons are detected by photo diodes. The reflector and the septa should prevent the optical photons from leaving the detector pixel.

Several effects have to be taken into account when simulating this kind of process in order to get the output signal of a detector:

- The interaction between incoming X-ray photons and the scintillator material depends on the photon energy and the material composition of the detector and its geometry.
- There are different types of interactions which may deflect or create photons on different paths. These escape photons may cause additional interaction events which may take place in another pixel (X-ray cross-talk).
- Optical photons may penetrate the septa and therefore be lost or reach the photo-diode of another pixel (optical cross-talk).
- The transport of optical photons may be delayed by defects within the scintillator material (afterglow)
- The read-out electronic noise influences the signal to noise ratio

Michael Balda and Joachim Hornegger are with the Friedrich-Alexander University, Erlangen, Germany

Stefan Wirth and Daniel Niederlöhner are with Siemens Healthcare, Forchheim, Germany

Björn Heismann is with the Friedrich-Alexander University, Erlangen, Germany and Siemens Healthcare, Forchheim, Germany

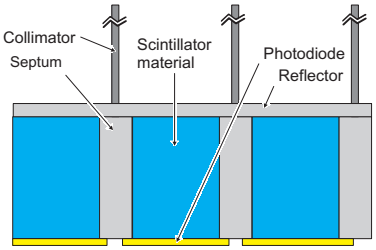

Fig. 1. Basic layout of a scintillator as used in CT

These effects are directly or indirectly influenced by the geometry of the scintillator pixels, for example by the ratio of septa and active pixel area or the pixel height. The introduced simulation can be used to investigate the influence of these detector properties on the resulting quality of the reconstructed CT-image.

II. Simulation

The effects mentioned in the previous section are usually modeled by an X-ray- and light photon-based simulation. This approach is very time consuming since the amount of photons to be dealt with is usually very large. We use precomputed interaction events and separate the X-ray photon interaction and the transport of optical photons [1]. The data is provided in look-up tables (LUTs), which have to be computed only once for a specific detector geometry and material composition. Figure 2a shows the components of the simulation. These components are described in the following:

a) X-ray photon interaction: The photon interaction LUT holds data of precomputed X-ray interaction events for a uniformly irradiated detector pixel. The incoming X-ray photons hit the detector orthogonally. Covering arbitrary angles of incidence is not necessary for the CT case. This data can be provided by a Monte-Carlo simulation of particle interactions like ROSI [2] or Geant4 [3], [4]. The events are grouped into energy bins with respect to the energy of the

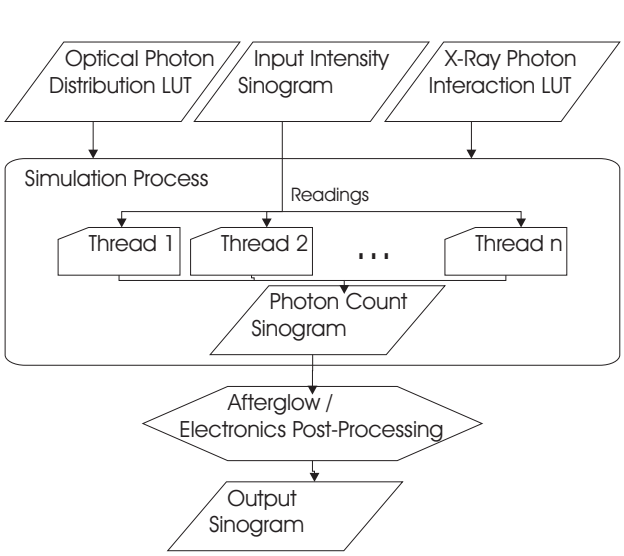

(a) Basic simulation layout

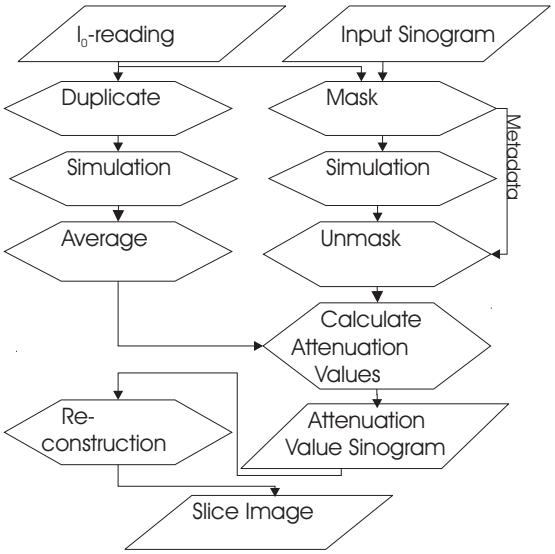

(b) Workflow for slice image generation with masking for complete CT scan simulation

Fig. 2. Signal flow diagrams for detection- and complete CT scan simulation

corresponding incoming photon. We chose to have one million events available for all energy bins of 5 keV width. One event contains an arbitrary amount of interaction data-sets, since an incoming photon might not interact at all or might produce one or more interactions. An interaction data-set contains the following entries:

- Relative 2D detector pixel location of the interaction (non-zero in case of X-ray cross-talk)
- Number of generated optical photons (depends on the deposited energy of the interaction)
- Discrete 3D location within the scintillator element. The location is quantized to a discrete voxel position $\mathbf{v}$ within the pixel.

Figure 3 visualizes the LUT-data for two energy bins at 25 keV and 100 keV. Figure 3a shows the interaction locations and the respective energy deposition of several thousand 100 keV events. The photon interction LUT stores the interactions positions in quantized form as 3D-voxel coordinates. Figures 3(b) and (c) show two histogramms of the energy deposition within the scintillator material with respect to the interaction voxel indices. For this case we used $20 \times 20 \times 20$ voxels in phi-, z- and depth-direction for each scintillator pixel. The figure only shows the central voxels with respect to the z-direction. This data is computed for a photon interaction LUT that contains 10^6 X-ray photons (events) per energy bin. Energy deposited within the septa is discarded and the corresponding interactions are not stored in the LUT as they do not contribute to the output signal. The figures show that most of the energy is deposited in the scintillator of the illuminated pixel and, as expected, the energy deposition decreases exponentially with increasing depth. The neighboring pixels show the energy deposition due to X-ray cross-talk as they are not exposed to direct radiation. Here the energy deposition does not show such a clear dependence on depth, but decreases with distace to the center pixel.

b) Optical photon distribution: The optical cross-talk is modeled as a set of two-dimensional distribution functions $d_{\mathbf{v}}(\mathbf{x_p})$ for each discrete position $\mathbf{v}$ within the pixel. $d_{\mathbf{v}}(\mathbf{x_p})$ yields the probability that an optical photon released at $\mathbf{v}$ reaches the photo-diode at relative pixel position $\mathbf{x_p}$. As the intensity of the optical cross-talk drops exponentially with the distance to the originating pixel, it is sufficient to limit $d_{\mathbf{v}}(\mathbf{x_p})$ to a small region. A significant amount of optical photons does not reach a photo-diode pixel, therefore $\sum_{\mathbf{x_p}} d_{\mathbf{v}}(\mathbf{x_p})$ is smaller than 1. The data needed for this look-up table can be acquired using a light transport simulation [5]. With this data we form a so called optical photon distribution LUT, which contains a distribution function for each voxel center of the interaction LUT.

The total amount of optical photons generated in one interaction is distributed over pixels within the neighborhood with the respective LUT-entries as weighting factors. Poisson noise is applied to the optical photon numbers of each event and pixel. Figure 4 shows the typical properties of this LUT by comparing the detection probabilities for some specific voxel locations. Figure 4a shows the probability distribution for the center voxel on a log scale. The influence of the interaction location on the optical cross-talk can be seen in the absolute

detection probablities as well as the amount of cross-talk in the respective neighboring pixels: Figure 4b shows only a slight shift in the detection probability if an optical photon is created on the very right or left edge of the scintillator pixel at the same depth. The influence of the depth of interaction is considerably larger (see Fig. 4c): Photons created far off the photo diode have a high cross-talk probablity and are less likely to be detected at all.

c) Input data: For a complete scan simulation the input sinogram contains data for all channels and readings. This data consists of mean values of incoming X-ray photons at specific energies. The input sinograms can be computed by an analytic projection tool like *NCAT4D* [6]. For this purpose geometric phantoms have to be defined. For each ray from the focal spot of the X-ray tube to the detector pixels the according lengths within the phantom materials are computed. The total attenuation for the ray can then be estimated using the attenuation coefficients of the phantom materials and the corresponding intersection lengths. These attenuations are applied to an appropriate tube spectrum. It contains the X-ray photon counts per energy. Information about how to acquire tube spectra can be found in [7].

d) Simulation process: The simulation consists of the following steps:

1) Get the mean number of incoming X-ray photons for each channel, reading and energy level
2) Apply Poisson distributed noise
3) For each X-ray photon, pick random event and get all interactions (Gives the number of created optical photons and voxel locations of interactions)
4) For each interaction: Distribute the optical photons to the according photo-diode pixels using the matching optical photon distribution LUT entries
5) Apply Poisson distributed noise to optical photon counts at photo-diode prior to adding to the output signal of the respective pixels

The result of this process are optical photon counts at each photo diode pixel.
The process can be parallelized for subsequent readings to utilize multiple processors and/or multi-core processors. The run-time of the simulation is linearly dependent of the total number of incoming X-ray photons of all detector channels and read-outs per channel. The energy distribution of the incoming X-ray photons can have a minor influence on the simulation run-time as the average number of interactions varies with X-ray photon energy.

e) Electronics and afterglow post-processing: Electronics properties like quantization or amplifier noise additionally influence the measurement. These effects can be modeled as a post-processing step on the photon count data. Scintillator afterglow is modeled as temporal cross-talk between subsequent measurements. It cannot be handled within the simulation process as it does not resolve temporal behavior. So if the simulation of afterglow effects is desired, it is treated in a post-processing step as well. It consists of convoluting the measurement signal of each channel at multiple readings with an appropriate impusle response function that models the afterglow characteristics. In this case, a sum of decaying exponential functions can be used. The model parameters can be acquired by measuring the afterglow characteristics of the scintillator material [8].

We use the following optional speed-up techniques:

f) Masking: The computation time is linearly dependent on the total amount of incoming X-ray photons. For simulating whole CT-scans most time is spent on simulating sinogram regions that are exposed to direct radiation even though these regions contain little information. In many cases the computation time can be reduced by masking those regions prior to simulation. This can be done by compairing the input sinogram with an i_0-reading which is only exposed to direct radiation. It is necessary to simulate at least one i_0-reading for a full scan simulaton, since it is needed to convert measured intensities into attenuation values. This enables us to unmask the result using the simulated i_0-reading. It is recommended to simulate multiple i_0-readings for two reasons: First of all a low-noise i_0-reading is needed to generate a sinogram of attenuation values from intensity values, secondly varying i_0-readings can be used for unmasking, otherwise the same noise pattern would repeat in the unmasked regions. Precomputed i_0-reading results may be re-used for later simulations with same detector geometry and X-ray tube settings. Figure 2b shows a diagram containing all necessary steps for a complete CT scan simulation including masking and i_0 simulation.

g) Total cross-talk simulation: The usage of a total cross-talk LUT offers the possibility to trade accuracy for speed. The total cross-talk LUT combines X-ray photon interaction and optical photon transport properties. It contains numbers of detected optical photons in a defined neighborhood around an illuminated pixel for a fixed amount of incoming X-ray photons. This LUT can be computed in advance from the photon interaciton LUT and the optical photon distribution LUT data for a very large amount of incoming X-ray photons. This is done separately for each energy bin to preserve the energy dependence of the input data. This LUT offers only one total optical photon distribution for each energy bin.
The usage of this LUT requires the following steps for each channel, reading and energy bin of the input data:

1) Retrieve the number of detected optical photons in each pixel within the neighborhood of the current channel (look-up in total cross-talk LUT)
2) For each pixel in this neighborhood: Scale this value with respect to the number of X-ray photons in the current energy bin of the input data
3) Apply Poisson noise
4) Add the resulting value of detected optical photons to the respective pixel signal of the output data

The decision for this using LUT or the spearated X-ray interaction and optical photon transport LUTs can be triggered with a threshold: If the amount of incoming X-ray photons exceeds the threshold within an energy bin, the scaled values of the total cross-talk LUT can be used to directly calculate the amount of optical photons reaching the neighboring photodiodes. This approach is several orders of magnitude faster than computing the optical cross-talk separately for each X-ray photon. Its time consumption is independent of the X-ray

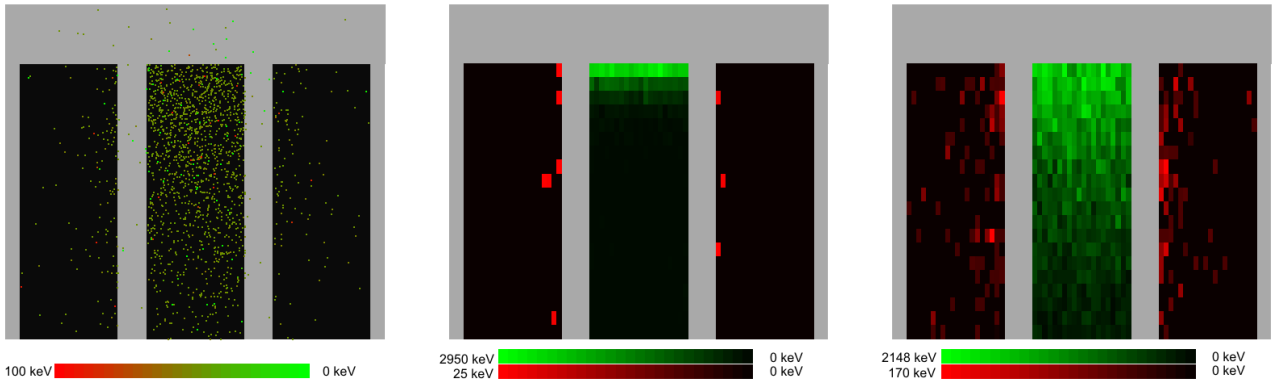

(a) (b) (c)

Fig. 3. (a) Interaction locations of 2500 X-ray photon events (100 keV) and excerpt of the histogramm of energy deposition within scintillator voxels for equidistributed irradiation of center pixel with monoenergetic X-ray photons. Central slice in z-direction is shown. (b) 25 keV photons, (c) 100 keV photons.

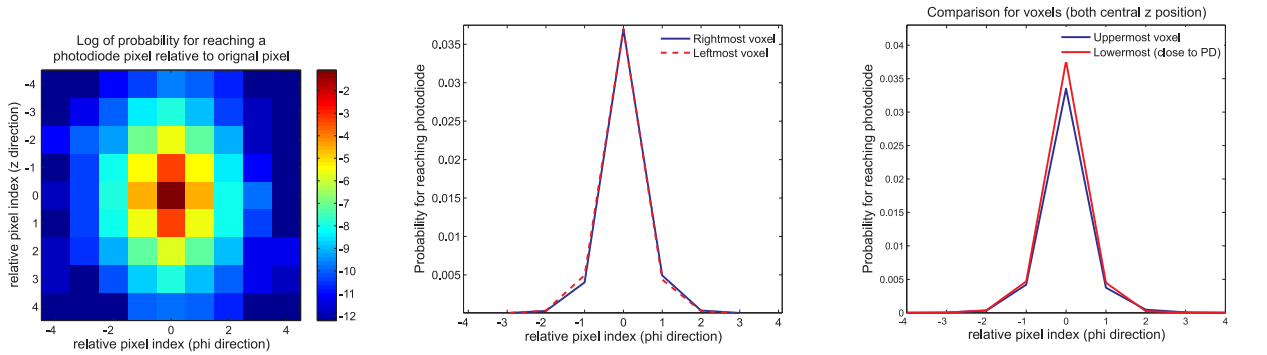

(a) Optical photon distributions for top center region of scintillator pixel

(b) Comparison between rightmost and leftmost voxel with respect to phi-direction (central depth- and z-coordinate)

(c) Comparison between topmost and bottommost voxel with respect to interaction depth (central phi- and z-coordiante)

Fig. 4. Optical photon distribution-LUT example and comparisons between voxel positions

flux and depends linearly on the number of detector channels and read-outs per channel. However, it does not offer the high precision of the approach using separated LUTs. The threshold value can be used to steer the trade-off between speed and precision.

III. Results

We evaluate two possible applications of this type of simulation: The estimation of the detector NPS and the image MTF. All results presented in the following section are based on simulations of Gd_2O_2S:Pr scintillators. The X-ray photon interaction events were precomputed using a proprietary particle interaction simulation.

Image MTF comparison: With this experiment we examine the principal possibility to conduct complete CT scan simulations with this simulation framework. A 672-channel detector of 64 rows with 1.3 mm phi-pitch and 1.1 mm z-pitch was simulated. The results were compared to measured data of a Siemens Sensation 64 CT-scanner. A high-contrast phantom was used (Catphan 500, `http://www.phantomlab.com/catphan.html`). The phantom contains inlays of line-patterns with increasing number of line pairs per cm (lp/cm). It is used the estimate the frequency resolution of the reconstructed image.

Figure 5a shows a comparison of measured and simulated image MTFs for a body reconstruction kernel. The average error of the simulated MTF in the range of 1 to 10 lp/cm is 3.68%. This kind of simulation, however, includes many parameters that are not related to the detector like tube and reconstruction properties. Therefore we performed further tests that focus on the detector properties.

Detector NPS estimation: In order to verify the simulation performance independently of the influence of other system parameters we compute the detector noise power spectrum (NPS) from simulated and measured data. The NPS can be computed from the detector signal resonse to an X-ray flat-field. It contains information on the signal noise level and the modulation transfer characteristics of the detector.
First we compare simulated NPS results of our look-up table-based approach with those of a fully single-photon based Monte-Carlo simulation. Both do not include electronics simulation. The later approach is very precise but extremely time consuming and therefore not feasible for most simulation scenarios. The detector NPS estimates from a flat-field image of 512×512 detector pixels and low intensity radiation

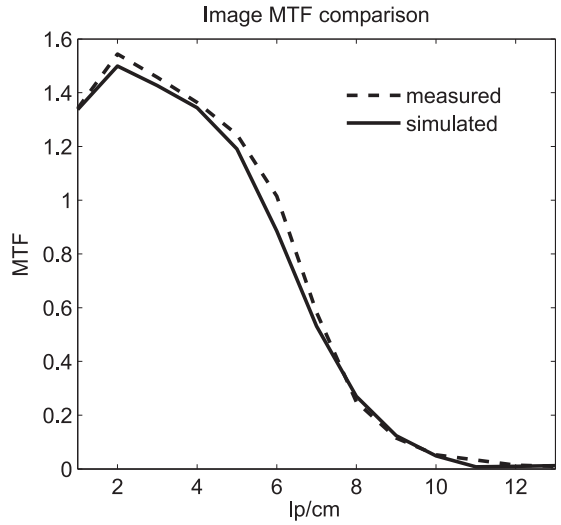

(a) Image MTF comparison

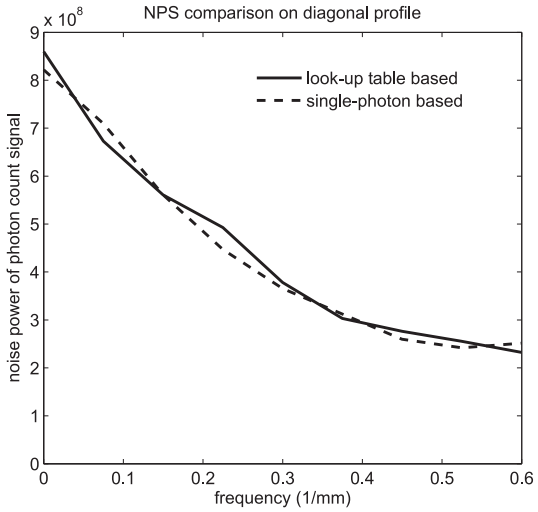

(b) Simulated NPS comparison

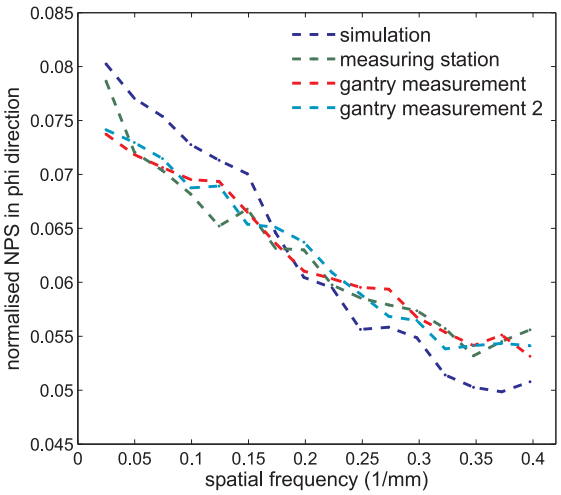

(c) NPS in phi-direction

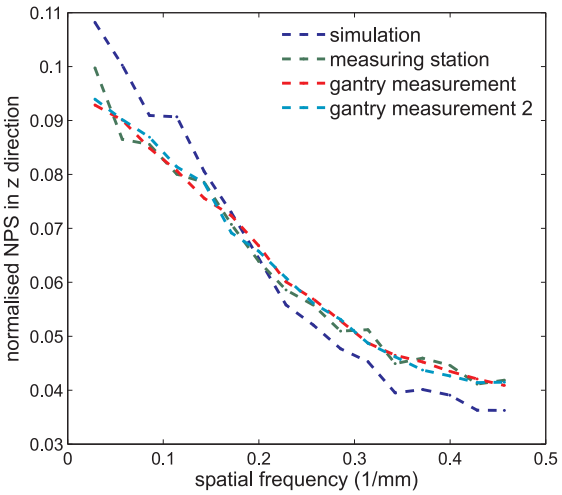

(d) NPS in z-direction

Fig. 5. (a) Image-MTF comparison; (b) detector NPS comparison (profile of 2D-NPS along diagonal of 1st quadrant) between proposed simulation and full scale Monte-Carlo simulation; (c) and (d) NPS comparison between simulation and different measurements in measuring station and CT gantry

are compared for both approaches. The simulation with our approach took 8:15 minutes on an Intel Core2Duo T5500 at 1.66 GHz with single-threaded simulation and total cross-talk optimization turned off (see Sec. II-0e for details). The average deviation of the NPS values is 3.06%. Figure 5b shows a comparison of a diagonal profile of the 2D-NPS. This approach is about 200 times faster than the full-scale simulation.

The second detector NPS evaluation compares measurements taken from the CT gantry and a detector measuring station and the simulation tool. The simulation includes electronics post-processing, total cross-talk optimization is turned off. The results are shown in Fig. 5(c) and (d). The NPS values between simulation and gantry measurement again show a good agreement with an average relative deviation of $5.23\,\%$ in phi-direction. Comparing the shapes of the NPS shows a faster drop off towards higher frequencies in the simulated NPS. This indicates a slight overestimation of the cross-talk.

IV. Conclusion

We have introduced a new type of detector simulation that combines the precision of a Monte-Carlo particle simulation with the performance that is necessary to cover realistic scenarios. We have successfully verified our approach against data measured with a CT scanner and a single-photon based Monte-Carlo simulation for two possible applications for this kind of simulation: Investigation of the effects of the detector on the MTF of the reconstructed image and detector NPS estimation. The results show that our look-up table based simulation models the detector performance appropriately to investigate its effects on CT image quality.

REFERENCES

[1] B. J. Heismann, K. Pham-Gia, W. Metzger, D. Niederloehner, and S. Wirth, "Signal transport in Computed Tomography detectors," *Nuclear Instruments and Methods in Physics Research Section A*, vol. 591, no. 1, pp. 28–33, 2008.

[2] J. Giersch, A. Weidemann, and G. Anton, "ROSI - an object-oriented and parallel-computing Monte Carlo simulation for X-ray imaging," *Nuclear Instruments and Methods in Physics Research*, vol. 509, no. 1-3, pp. 151–156, August 2003.

[3] S. Agostinelli *et al.*, "G4 - a simulation toolkit," *Nuclear Instruments and Methods in Physics Research*, vol. 506, no. 3, pp. 250–303, July 2003.

[4] J. Allison *et al.*, "Geant4 developments and applications," *IEEE Transactions on Nuclear Science*, vol. 53, no. 1, pp. 270–278, Februar 2006.

[5] S. Wirth, W. Metzger, K. Pham-Gia, and B. J. Heismann, "Impact of Photon Transport Properties on the Detection Efficiency of Scintillator Arrays," *IEEE Nuclear Science Symposium Conference*, no. M11-212, pp. 2602–2603, 2003.

[6] W. P. Segars, B. M. W. Tsui, E. C. Frey, and E. K. Fishman, "Extension of the 4D NCAT phantom to dynamic X-ray CT simulation," *IEEE Nuclear Science Symposium Conference Record*, vol. 5, pp. 3195–3199, 2003.

[7] H. Aichinger, J. Dierker, S. Joite-Barfuß, and M. Säbel, *Radiation Exposure and Image Quality in X-Ray Diagnostic Radiology*. Berlin: Springer-Verlag, 2004.

[8] P. Lecoq, A. Annenkov, A. Gektin, M. Korzhik, and C. Pedrini, *Inorganic Scintillators for Detector Systems*. Berlin: Springer-Verlag, 2006.